N O T I C E

THIS DOCUMENT HAS BEEN REPRODUCED FROM MICROFICHE. ALTHOUGH IT IS RECOGNIZED THAT CERTAIN PORTIONS ARE ILLEGIBLE, IT IS BEING RELEASED IN THE INTEREST OF MAKING AVAILABLE AS MUCH INFORMATION AS POSSIBLE

NI

Simplified Solution for Stresses and Deformation

Bernard J. Hamrock
Lewis Research Center
Cleveland, Ohio

and

David E. Brewe
Propulsion Laboratory
AVRADCOM Research and Technology Laboratories
Lewis Research Center
Cleveland, Ohio

NASA

SIMPLIFIED SOLUTION FOR STRESSES AND DEFORMATIONS

Bernard J. Hamrock and David E. Brewe[*]

National Aeronautics and Space Administration

Lewis Research Center

Cleveland, Ohio 44135

SUMMARY

A shortcut to the classical Hertzian solution for local stress and deformation of two elastic bodies in contact is presented. The shortcut is accomplished by using simplified forms for the ellipticity and for the complete elliptic integrals of the first and second kinds as a function of the geometry. Thus the interdependence of these variables can be uncoupled, and the resulting transcendental equation, which must be solved through use of the computer or design charts, avoided.

Simplified formulas that make the elastic deformation at the center of contact easy to calculate have been previously reported by the authors. However, the range of applicability was limited to ellipticities greater than or equal to 1. This paper extends the range of validity to include ellipticities less than 1, that is, where the semimajor axis in the elliptical contact lies in a direction parallel to the rolling direction rather than being perpendicular as in previous studies. Furthermore an auxiliary shear stress parameter is expressed in simplified form as a function of the geometry. This enables a shortcut calculation to be made for the location and magnitude of the maximum subsurface shear stress.

E-905

---

[*]Propulsion Laboratory, AVRADCOM Research and Technology Laboratories.

INTRODUCTION

The classical Hertzian solution for deformation requires the calcula-
tion of the ellipticity parameter k and the complete elliptic integrals of
the first and second kinds, $\mathscr{F}$ and $\mathscr{E}$, respectively. Simplifying expres-
sions for k, $\mathscr{F}$, and $\mathscr{E}$ as a function of the radius ratio α were pre-
sented by Brewe and Hamrock (1977) using a curve-fit analysis. With these
expressions the deformation at the center of the contact δ could be deter-
mined, with a slight sacrifice in accuracy, without involved mathematical
methods or the use of design charts. The simplifying expressions were use-
ful for radius ratios ranging from circular point contact to a near line
contact normal to the rolling direction (i.e., $1.0 \leq \alpha \leq 35$). However,
there are a number of applications for which the semimajor axis in the
elliptical contact lies in a direction parallel to the rolling direction,
resulting in $\alpha < 1$. In local deformation due to asperity-asperity interac-
tion, the radius ratio can range from much less than 1 (Patir and Cheng,
1978) to infinity. For many gear and rolling-element bearing applications
the "run-in" surface becomes anisotropic and the radius ratio is generally
less than 1 for local asperity contact. Other examples where α may be
less than 1 are (1) Navikov gear contacts, (2) locomotive wheel-rail con-
tact, and (3) roller-flange contact in an axially loaded roller bearing.
Therefore the elliptical-contact deformation and stresses to be presented in
this paper are applicable for any contact ranging from something similar to
a disk rolling on a plate (radius ratio $\alpha = 0.03$) to a ball-on-plate con-
tact ($\alpha = 1$) to a contact approaching a nominal line contact ($\alpha \rightarrow 100$) such
as a barrel-shaped roller against a plate.

Thus far, we have limited our consideration to the use of the simpli-
fied formulas in determining the elliptical-contact deformation. In this

paper we further illustrate their applicability in calculating surface stress as well as subsurface stress, which is important to the determination of fatigue life in rolling-element bearings.

SYMBOLS

A	solid A
B	solid B
D_x, D_y	diameters of contact ellipse along x and y directions, respectively (cm)
E	modulus of elasticity (N/cm^2)
E'	$2 \left/ \left(\dfrac{1 - \nu_A^2}{E_A} + \dfrac{1 - \nu_B^2}{E_B} \right) \right.$ (N/cm^2)
$\mathcal{E}$	complete elliptic integral of second kind
$\bar{\mathcal{E}}$	approximate value of $\mathcal{E}$ using curve-fit equation
F	applied load (N)
$\mathcal{F}$	complete elliptic integral of first kind
$\bar{\mathcal{F}}$	approximate value of $\mathcal{F}$ using curve-fit equation
k	(D_y/D_x), ellipticity
$\bar{k}$	approximate value of k using curve-fit equation
R_x	effective radius of curvature in x-plane (cm)
R_y	effective radius of curvature in y-plane (cm)
$1/R$	$(1/R_x + 1/R_y)$, curvature sum (cm^{-1})
r_{ax}, r_{ay}	principal radii of solid a (cm)
r_{bx}, r_{by}	principal radii of solid b (cm)
t	auxiliary parameter
$\bar{t}$	auxiliary parameter using curve-fit equation
x_0	location along x-axis (rolling direction) of maximum subsurface shear stress (cm)
$\bar{x}_0$	calculated value of x_0 using approximate formula (cm)

3

z_0 depth of maximum subsurface shear stress in x-z plane (cm)

$\bar{z}_0$ calculated value of z_0 using approximate formula (cm)

Γ curvature difference

δ elliptical-contact deformation at center of contact (cm)

$\bar{\delta}$ elliptical-contact deformation calculated by using approximate formulas (cm)

σ_{max} maximum Hertzian stress (N/cm^2)

$\bar{\sigma}_{max}$ maximum Hertzian stress calculated by using approximate formulas (N/cm^2)

τ_0 maximum subsurface orthogonal shear stress (N/cm^2)

$\bar{\tau}_0$ maximum subsurface orthogonal shear stress using approximate formulas (N/cm^2)

CONFORMAL AND NONCONFORMAL SURFACES

Hydrodynamic lubrication is generally characterized by surfaces that are conformal. That is, the surfaces fit snugly into each other with a high degree of geometrical conformity, so that the load is carried over a relatively large area. Furthermore the load-carrying surface area remains essentially constant while the load is increased. Fluid-film journal and slider bearings are conformal surfaces. ьп journal bearings the radial clearance between the shaft and the bearing is typically one-thousandth of the shaft diameter; in slider bearings the inclination of the bearing surface to the runner is typically one part in a thousand.

Many machine elements have contacting surfaces that do not conform to each other very well. The full burden of the load must then be carried by a very small contact area. In general, the contact areas between nonconformal surfaces enlarge considerably with increasing load but are still small compared with the contact areas between conformal surfaces. Some examples of

4

these nonconformal surfaces are mating gear teeth, cams and followers, and rolling-element bearings.

The load per unit area in conformal bearings is relatively low, typically only 1 MN/m^2 and seldom over 7 MN/m^2. By contrast, the load per unit area in nonconformal contacts, such as those that exist in ball bearings, will generally exceed 700 MN/m^2 even at modest applied loads. These high pressures result in elastic deformation of materials such that the elliptical contact areas are formed for load support. The present paper develops simple solutions for the stresses and deformations in nonconformal contacts.

CURVATURE SUM AND DIFFERENCE

The undeformed geometry of contacting solids can be represented in general terms by two ellipsoids. The two solids with different radii of curvature in a pair of principal planes (x and y) passing through the contact between the solids make contact at a single point under the condition of zero applied load. Such a condition is called point contact and is shown in figure 1, where the radii of curvature are denoted by r's. It is assumed throughout the paper that convex surfaces, as shown in figure 1, exhibit positive curvature and concave surfaces, negative curvature. Therefore, if the center of curvature lies within the solid, the radius of curvature is positive; if the center of curvature lies outside the solid, the radius of curvature is negative. It is important to note that, if coordinates x and y are chosen such that

$$\frac{1}{r_{ax}} + \frac{1}{r_{bx}} \geq \frac{1}{r_{ay}} + \frac{1}{r_{by}} \tag{1}$$

coordinate x then determines the direction of the semiminor axis of the contact area when a load is applied and y, the direction of the semimajor

axis. The direction of motion is always considered to be along the x-axis. For those situations in which the principal curvature planes of the two contacting bodies are not coincident, refer to Timoshenko and Goodier (1970).

The curvature sum and difference, which are quantities of some importance in the analysis of contact stresses and deformation, are

$$\frac{1}{R} = \frac{1}{R_x} + \frac{1}{R_y} \tag{2}$$

$$\Gamma = R \left(\frac{1}{R_x} - \frac{1}{R_y} \right) \tag{3}$$

where

$$\frac{1}{R_x} = \frac{1}{r_{ax}} + \frac{1}{r_{bx}} \tag{4}$$

$$\frac{1}{R_y} = \frac{1}{r_{ay}} + \frac{1}{r_{by}} \tag{5}$$

Equations (4) and (5) effectively redefine the problem of two ellipsoidal solids approaching one another in terms of an equivalent ellipsoidal solid of radii R_x and R_y approaching a plane.

The radius ratio α is defined as

$$\alpha = \frac{R_y}{R_x} \tag{6}$$

Thus, if equation (1) is satisfied, then α is greater than or equal to 1; and if it is not satisfied, α is less than 1.

SURFACE STRESSES AND DEFORMATION

When two elastic solids are brought together under a load, a contact area develops, the shape and size of which depend on the applied load, the elastic properties of the materials, and the curvatures of the surfaces.

When the two solids shown in figure 1 have a normal load applied to them, the shape of the contact area is elliptical. It has been common to refer to elliptical contacts as point contacts, but since this paper deals mainly with loaded contacts, the term elliptical contact is adopted. For the special case where $r_{ax} = r_{ay}$ and $r_{bx} = r_{by}$, the resulting contact is a circle rather than an ellipse. Where r_{ay} and r_{by} are both infinite, the initial line contact develops into a rectangle when load is applied.

The ellipticity parameter k is defined as the elliptical-contact diameter in the y-direction (transverse direction) divided by the elliptical-contact diameter in the x-direction (direction of motion) or

$$k \equiv \frac{D_y}{D_x} \tag{7}$$

If equation (1) is satisfied and $\alpha \geq 1$, the orientation of the contact ellipse will have the major diameter transverse to the direction of motion, and consequently $k \geq 1$. Otherwise, the major diameter would lie along the direction of motion with both $\alpha \leq 1$ and $k \leq 1$. To avoid confusion, the commonly used solutions to the surface deformation and stresses are presented only for the case in which $\alpha \geq 1$. The simplified solutions are presented and then their application for $\alpha < 1$ is discussed.

Harris (1966) has shown that the ellipticity parameter can be written as a transcendental equation relating the curvature difference (eq. (3)) and the elliptic integrals of the first $\mathscr{F}$ and second $\mathscr{E}$ kinds as

$$k = \frac{2\mathscr{F} - \mathscr{E}(1 + \Gamma)^{1/2}}{\mathscr{E}(1 - \Gamma)} \tag{8}$$

where

$$\mathscr{F} = \int_0^{\pi/2} \left[1 - \left(1 - \frac{1}{k^2}\right) \sin^2\phi \right]^{-1/2} d\phi \qquad (9)$$

$$\mathscr{E} = \int_0^{\pi/2} \left[1 - \left(1 - \frac{1}{k^2}\right) \sin^2\phi \right]^{1/2} d\phi \qquad (10)$$

A one-point iteration method that was adopted by Hamrock and Anderson (1973) can be used to obtain the ellipticity parameter, where

$$k_{n+1} \approx k_n \qquad (11)$$

The iteration process is normally continued until k_{n+1} differs from k_n by less than 1×10^{-7}. Note that the ellipticity parameter is a function of the radii of curvature of the solids only:

$$k = f(r_{ax}, r_{bx}, r_{ay}, r_{by}) \qquad (12)$$

That is, as the load increases, the semi-axes in the x and y directions of the contact ellipse increase proportionately to each other, so the ellipticity parameter remains constant.

Figure 2 shows the ellipicity parameter and the elliptic integrals of the first and second kinds for a range of the curvature ratio R_y/R_x usually encountered in concentrated contacts.

When the ellipcity parameter k, the normal applied load F, Poisson's ratio v, and the modulus of elasticity E of the contacting solids are known, the major and minor axes of the contact ellipse and the maximum deformation at the center of the contact can be written from the analysis of Hertz (1881) as

$$D_y = 2 \left(\frac{6k^2 \mathscr{E} FR}{\pi E'} \right)^{1/3} \qquad (13)$$

8

$$D_x = 2\left(\frac{6\mathscr{S}FR}{\pi kE'}\right)^{1/3} \tag{14}$$

$$\delta = \mathscr{F}\left[\left(\frac{9}{2\mathscr{S}R}\right)\left(\frac{F}{\pi kE'}\right)^2\right]^{1/3} \tag{15}$$

where

$$E' = \frac{2}{\dfrac{1-\nu_a^2}{E_a} + \dfrac{1-\nu_b^2}{E_b}} \tag{16}$$

In these equations, D_y and D_x are proportional to $F^{1/3}$ and δ is proportional to $F^{2/3}$.

The maximum Hertzian stress at the center of contact can also be determined by using equations (13) and (14) and

$$\sigma_{max} = \frac{6F}{\pi D_y D_x} \tag{17}$$

SUBSURFACE STRESSES

Fatigue cracks usually start at a certain depth below the surface in planes parallel to the direction of rolling. Because of this, special attention must be given to the shear stress amplitude in this plane Furthermore a maximum shear stress is reached at a certain depth below the surface. The analysis used by Lundberg and Palmgren (1947) is used here to define this stress.

The stresses are referred to a rectangular coordinate system with its origin at the center of the contact, its z-axis coinciding with the interior normal of the body considered, its x-axis in the direction of rolling, and its y-axis perpendicular to the rolling direction. In the analysis that follows, it is assumed that $y = 0$.

From Lundberg and Palmgren (1947) the following equations can be written:

$$\tau_{zx} = \frac{6F}{\pi} \frac{\cos^2\phi \, \sin\phi \, \sin\gamma}{\left(D_y^2 \tan^2\gamma + D_x^2 \cos^2\phi\right)} \tag{18}$$

$$x = \frac{1}{2} \sqrt{D_x^2 + D_y^2 \tan^2\gamma} \, \sin\phi \tag{19}$$

$$z = \frac{D_y}{2} \tan\gamma \cos\phi \tag{20}$$

where ϕ and γ are auxiliary parameters used in place of the coordinate set (x,z). They are defined so as to satisfy the relationship for a confocal ellipsoid to the pressure ellipse (for further details see Hertz, 1881, and Lundberg and Palmgren, 1447). The maximum shear stress amplitude is defined as

$$\tau_0 = \left|\tau_{zx}\right|_{max}$$

The amplitude of the shear stress τ_0 is obtained from

$$\frac{\partial\tau_{zx}}{\partial\phi} = 0$$

$$\frac{\partial\tau_{zx}}{\partial\gamma} = 0$$

For the point of maximum shear stress

$$\tan^2\phi = t \tag{21}$$

$$\tan^2\gamma = t - 1 \tag{22}$$

$$\frac{D_x}{D_y} = \sqrt{(t^2 - 1)(t - 1)} \tag{23}$$

The position of the maximum point is determined by

$$z_0 = \zeta^* \frac{D_x}{2} \tag{24}$$

$$x_0 = \pm \eta^* \frac{D_x}{2} \tag{25}$$

where

$$\zeta^* = \frac{1}{(t + 1) \sqrt{2t - 1}} \tag{26}$$

$$\eta^* = \frac{t}{t + 1} \sqrt{\frac{2t + 1}{2t - 1}} \tag{27}$$

Furthermore the magnitude of the maximum shear stress is given by

$$\tau_0 = \sigma_{max} \frac{\sqrt{2t - 1}}{2t(t + 1)} \tag{28}$$

It should be emphasized that τ_0 represents the maximum half-amplitude of the subsurface orthogonal shear stress and is not to be confused with the maximum subsurface shear stress that occurs below the center of contact on the plane oriented 45° to the surface. The Lundberg-Palmgren prediction of fatigue life is based on the calculation of τ_0 and was limited to cross sections lying in the plane of symmetry ɔ the roller path (y = 0).

SIMPLIFIED SOLUTIONS FOR α > 1

The classical Hertzian solution presented in the previous section requires the calculation of the ellipicity parameter k and the complete elliptic integrals of the first and second kinds $\mathscr{F}$ and $\mathscr{E}$. This entails finding a solution to a transcendental equation relating k, $\mathscr{F}$, and $\mathscr{E}$ to the geometry of the contacting solids, as expressed in equation (8). This

11

is usually accomplished by some iterative numerical procedure, as described by Hamrock and Anderson (1973), or with the aid of charts, as shown by Jones (1946).

Table 1 shows various values of radius-of-curvature ratios and corresponding values of k, $\mathscr{F}$, and $\mathscr{E}$ obtained from the numerical procedure given in Hamrock and Anderson (1973). For the set of pairs of data $[(k_i, \alpha_i), i = 1, 2, \ldots, 26]$, a power fit using a linear regression by the method of least squares resulted in the following equation:

$$\bar{k} = \alpha^{2/\pi} \qquad \text{for } \alpha \geq 1 \qquad (29)$$

The asymptotic behavior of $\mathscr{E}$ and $\mathscr{F}$ ($\alpha \to 1$ implies $\mathscr{E} \to \mathscr{F} \to \pi/2$, and $\alpha \to \infty$ implies $\mathscr{F} \to \infty$ and $\mathscr{E} \to 1$) was suggestive of the type of functional dependence that $\bar{\mathscr{E}}$ and $\bar{\mathscr{F}}$ might follow. As a result, an inverse and logarithmic curve fit was tried for $\bar{\mathscr{E}}$ and $\mathscr{F}$, respectively. The following expressions provided excellent curve fits:

$$\bar{\mathscr{E}} = 1 + \frac{q}{\alpha} \qquad \text{for } \alpha \geq 1 \qquad (30)$$

where

$$q = \frac{\pi}{2} - 1 \qquad (31)$$

and

$$\bar{\mathscr{F}} = \frac{\pi}{2} + q \ln \alpha \qquad \text{for } \alpha \geq 1 \qquad (32)$$

Values of $\bar{k}$, $\bar{\mathscr{E}}$, and $\bar{\mathscr{F}}$ are presented in table 1 and compared with the numerically determined values of k, $\mathscr{E}$, and $\mathscr{F}$. Table 1 also gives the percentage of error determined as

$$e = \frac{(\bar{z} - z)100}{z} \tag{33}$$

where

$$z = \{k, \, \ell, \, \mathcal{F}\} \tag{34}$$

$$\bar{z} = \{\bar{k}, \, \bar{\ell}, \, \bar{\mathcal{F}}\} \tag{35}$$

Table 2 shows various values of radius-of-curvature ratios and corresponding values of D_y, D_x, σ_{max}, and α obtained exactly. Also shown in table 2 are the appropriate values $\bar{D}_y$, $\bar{D}_x$, $\bar{\sigma}_{max}$, and $\bar{\alpha}$ obtained from using equations (30) to (32) in conjunction with equations (13) to (15) and equation (28). The percentage of error as determined by equation (33) is also given in table 2. The agreement between the exact and approximate solutions is indeed quite good.

Table 3 shows various values of radius-of-curvature ratios and corresponding values of the auxiliary parameter t used in calculating the position and value of maximum subsurface orthogonal shear stress. For the set of pairs of data $[(t_i, \alpha_i), i = 1, 2, \ldots, 44]$ the following simplified formula was obtained:

$$\bar{t} = 1 + 0.16 \, \text{csch} \, \frac{\bar{k}}{2} \tag{36}$$

The position and value of maximum subsurface orthogonal shear stress corresponding to the auxiliary parameter are given in table 3. The percentage of error e is given for each of these values. The agreement between the exact and the approximate values of t is quite good. Once the value of the auxiliary parameter t is determined, the position and value of maximum subsurface orthogonal shear stress can readily be calculated.

13

SIMPLIFIED SOLUTIONS FOR $0.01 \leq \alpha \leq 1$

Table 4 gives the simplified equations for conditions where $0.01 \leq \alpha \leq 100$. Recall that $\alpha \geq 1$ implies $k \geq 1$ and equation (1) is satisfied and that $0 < \alpha < 1$ implies $0 < k < 1$ and equation (1) is not satisfied. It is important to make the proper evaluation of α since it has a great significance in the outcome of the simplified equations. It is also important to realize that the reciprocal of α produces the same values of the various parameters given in tables 1 and 2 as produced by α for a given curvature $1/R$.

Figure 3 shows three diverse situations in which the simplified equations can be usefully applied. The locomotive wheel on a rail (fig. 3(a)) illustrates an example in which the ellipticity k and radius ratio α are less than 1. The ball rolling against a flat plate (fig. 3(b)) provides pure circular contact (i.e., $\alpha = k = 1.00$). Figure 3(c) shows how the contact ellipse is formed in the ball – outer-ring contact of a ball bearing. Here the semimajor axis is normal to the direction of rolling and consequently α and k are greater than 1. The detailed geometry and the values from the calculations that can be made using the simplified formulas are given in table 5 for each of these configurations. In using these formulas it is important to pay attention to the sign of the curvatures. Note that the outer race in figure 3(c) is a concave surface and so the sign is negative.

SUMMARY OF RESULTS

An alternative approach has been presented for the classical Hertzian solution for local stress and deformation of two elastic bodies in contact. Simplified formulas that use curve-fit analysis are given in terms of the radius ratio α for the ellipticity k and for the complete elliptic

integrals, $\mathscr{F}$ and $\mathscr{E}$, of the first and second kinds, respectively. Thus their inter-dependence can be uncoupled, and solution of the resulting transcendental equation avoided. Simplified equations were developed that permit a more direct and easy approach to the calculation of the elliptical-contact deformation and maximum Hertzian stress. In addition, a curve-fit analysis was used to derive a simplified formula for an auxiliary stress parameter t as a function of the radius ratio α. This eliminated having to solve a cubic equation for t as a function of k. Thus the simplified formula for t, together with the simplified formulas for stresses and deformations, permits a direct and easy calculation of the location and magnitude of the maximum subsurface orthogonal shear stress. Therefore the elliptical-contact deformation and stresses are presented that are applicable for any contact ranging from a disk rolling on a plate (radius ratio $\alpha = 0.03$) to a ball-on-plate contact ($\alpha = 1$) to a contact approaching a nominal line contact ($\alpha \to 100$) such as a barrel-shaped roller against a plate.

REFERENCES

Brewe, D. E.; and Hamrock, B. J. (1977): Simplified Solution for Elliptical-Contact Deformation Between Two Elastic Solids. J. Lubr. Technol. vol 99, no. 4, 485-487.

Hamrock, B. J.; and Anderson, W. J. (1973): Analysis of an Arched Outer-Race Ball Bearing Considering Centrifugal Forces. J. Lubr. Technol., vol. 95, no. 3, 265-276.

Harris, Tedric A. (1966): Rolling Bearing Analysis. John Wiley & Sons, Inc. 1966.

Hertz, H. (1881): The Contact of Elastic Solids. J. Reine Angew. Math., vol. 92, 156-171.

Jones, A. B. (1946): Analysis of Stresses and Deflections; New Departure Engineering Data, Vol. I and II. General Motors, Inc.

Lundberg, G.; Palmgren A. (1947): Dynamic Capacity of Rolling Bearings. Acta Polytech., Mech. Eng. Sci., vol. 1, no. 3, 6-9.

Patir, Nadir; and Cheng, H. S. (1978): An Average Flow Model for Determining Effects of Three-Dimensional Roughness on Partial Hydrodynamic Lubrication. J. of Lubr. Technol., vol. 100, no. 1, 12-17.

Timoshenko, S. P.; and Goodier, J. N. (1970): Theory of Elasticity (Third Edition). McGraw-Hill Book Co., p. 415.

TABLE 1. - COMPARISON OF THE NUMERICALLY DETERMINED VALUES WITH THE CURVE FIT

VALUES FOR THE GEOMETRICALLY DEPENDENT VARIABLES

$[R_x = 1.0\ cm]$

RADIUS OF CURVATURE RATIO, α	ELLIPTICITY			COMPLETE ELLIPTIC INTEGRAL OF FIRST KIND			COMPLETE ELLIPTIC INTEGRAL OF SECOND KIND		
	k	$\bar{k}$	PERCENT ERROR, e	$\mathscr{F}$	$\bar{\mathscr{F}}$	PERCENT ERROR, e	$\mathscr{E}$	$\bar{\mathscr{E}}$	PERCENT ERROR, e
1.0000	1.0000	1.0000	0.00	1.5708	1.5708	0.00	1.5708	1.5708	0.00
1.2500	1.1604	1.1526	0.66	1.6897	1.6982	-0.50	1.4643	1.4566	0.52
1.5000	1.3101	1.2945	1.19	1.7898	1.8022	-0.70	1.3911	1.3805	0.76
1.7500	1.4514	1.4280	1.61	1.8761	1.8902	-0.75	1.3378	1.3262	0.87
2.0000	1.5858	1.5547	1.96	1.9521	1.9664	-0.73	1.2972	1.2854	0.91
3.0000	2.0720	2.0125	2.87	2.1883	2.1979	-0.44	1.2002	1.1903	0.83
4.0000	2.5007	2.4170	3.35	2.3595	2.3621	-0.11	1.1506	1.1427	0.69
5.0000	2.8902	2.7860	3.61	2.4937	2.4895	0.17	1.1205	1.1142	0.57
6.0000	3.2505	3.1289	3.74	2.6040	2.5935	0.40	1.1004	1.0951	0.48
7.0000	3.5878	3.4515	3.80	2.6975	2.6815	0.59	1.0859	1.0815	0.40
8.0000	3.9065	3.7577	3.81	2.7786	2.7577	0.75	1.0751	1.0713	0.35
9.0000	4.2096	4.0503	3.78	2.8502	2.8250	0.88	1.0666	1.0634	0.30
10.0000	4.4994	4.3313	3.74	2.9142	2.8851	1.00	1.0599	1.0571	0.26
15.0000	5.7996	5.6069	3.32	3.1603	3.1165	1.38	1.0397	1.0381	0.15
20.0000	6.9287	6.7338	2.81	3.3342	3.2807	1.60	1.0296	1.0285	0.10
25.0000	7.9440	7.7617	2.29	3.4685	3.4081	1.74	1.0236	1.0228	0.07
30.0000	8.8762	8.7170	1.79	3.5779	3.5122	1.84	1.0196	1.0190	0.05
35.0000	9.7442	9.6158	1.32	3.6700	3.6002	1.90	1.0167	1.0163	0.04
40.0000	10.5605	10.4689	0.87	3.7496	3.6764	1.95	1.0146	1.0143	0.03
45.0000	11.3340	11.2841	0.44	3.8196	3.7436	1.99	1.0129	1.0127	0.02
50.0000	12.0711	12.0670	0.03	3.8821	3.8038	2.02	1.0116	1.0114	0.02
60.0000	13.4557	13.5521	-0.72	3.9898	3.9078	2.06	1.0096	1.0095	0.01
70.0000	14.7430	14.9495	-1.40	4.0806	3.9958	2.08	1.0082	1.0082	0.01
80.0000	15.9522	16.2759	-2.03	4.1590	4.0720	2.09	1.0072	1.0071	0.01
90.0000	17.0969	17.5432	-2.61	4.2280	4.1393	2.10	1.0064	1.0063	0.00
100.0000	18.1871	18.7603	-3.15	4.2895	4.1994	2.10	1.0057	1.0057	0.00

TABLE 2. - DEFORMATION AND SURFACE STRESS VARIABLES CALCULATED BOTH NUMERICALLY AND WITH SIMPLIFIED FORMULAS

$$[E' = 2.1972 \times 10^{7} \text{ N/cm}^2; \quad F = 4.448 \text{ N}; \quad R_x = 1.0 \text{ cm}]$$

RADIUS OF CURVATURE RATIO, α	MAJOR AND MINOR AXIS OF ELLIPTICAL CONTACT (cm.)						MAXIMUM HERTZ STRESS (N/cm²)			DEFORMATION AT CENTER OF CONTACT (cm.)		
	D_y	$\bar{D}_y$	PERCENT ERROR, e	D_x	$\bar{D}_x$	PERCENT ERROR, e	σ_{max}	$\bar{\sigma}_{max}$	PERCENT ERROR, e	δ	$\bar{\delta}$	PERCENT ERROR, e
1.0000	0.0134	0.0134	0.00	0.0134	0.0134	0.00	0.470E 05	0.470E 05	-0.00	0.452E-04	0.452E-04	0.00
1.2500	0.0150	0.0149	0.62	0.0129	0.0129	-0.05	0.437E 05	0.440E 05	-0.57	0.435E-04	0.440E-04	-1.12
1.5000	0.0164	0.0163	1.05	0.0125	0.0126	-0.14	0.413E 05	0.416E 05	-0.91	0.421E-04	0.429E-04	-1.76
1.7500	0.0177	0.0175	1.37	0.0119	0.0122	-0.25	0.393E 05	0.398E 05	-1.13	0.410E-04	0.419E-04	-2.15
2.0000	0.0189	0.0186	1.61	0.0114	0.0119	-0.36	0.378E 05	0.383E 05	-1.28	0.400E-04	0.409E-04	-2.38
3.0000	0.0229	0.0224	2.19	0.0110	0.0111	-0.70	0.337E 05	0.342E 05	-1.54	0.370E-04	0.380E-04	-2.69
4.0000	0.0261	0.0255	2.47	0.0104	0.0105	-0.91	0.312E 05	0.317E 05	-1.61	0.349E-04	0.359E-04	-2.64
5.0000	0.0289	0.0281	2.60	0.0100	0.0101	-1.04	0.294E 05	0.299E 05	-1.62	0.334E-04	0.342E-04	-2.50
6.0000	0.0314	0.0305	2.66	0.0096	0.0098	-1.12	0.281E 05	0.285E 05	-1.60	0.321E-04	0.329E-04	-2.32
7.0000	0.0336	0.0327	2.68	0.0094	0.0095	-1.16	0.270E 05	0.275E 05	-1.57	0.311E-04	0.317E-04	-2.15
8.0000	0.0356	0.0346	2.67	0.0091	0.0092	-1.19	0.262E 05	0.266E 05	-1.54	0.302E-04	0.308E-04	-1.97
9.0000	0.0375	0.0365	2.64	0.0089	0.0090	-1.19	0.255E 05	0.258E 05	-1.50	0.294E-04	0.299E-04	-1.80
10.0000	0.0392	0.0382	2.59	0.0087	0.0088	-1.18	0.248E 05	0.252E 05	-1.46	0.287E-04	0.292E-04	-1.64
15.0000	0.0466	0.0456	2.28	0.0080	0.0081	-1.08	0.227E 05	0.229E 05	-1.24	0.262E-04	0.264E-04	-0.92
20.0000	0.0526	0.0516	1.92	0.0076	0.0077	-0.92	0.213E 05	0.215E 05	-1.02	0.245E-04	0.246E-04	-0.32
25.0000	0.0577	0.0568	1.56	0.0073	0.0073	-0.75	0.203E 05	0.204E 05	-0.82	0.232E-04	0.232E-04	-0.19
30.0000	0.0622	0.0614	1.22	0.0070	0.0070	-0.59	0.195E 05	0.196E 05	-0.64	0.222E-04	0.221E-04	-0.63
35.0000	0.0662	0.0656	0.89	0.0068	0.0068	-0.43	0.189E 05	0.190E 05	-0.47	0.214E-04	0.212E-04	1.02
40.0000	0.0699	0.0695	0.59	0.0066	0.0066	-0.28	0.184E 05	0.184E 05	-0.31	0.207E-04	0.205E-04	1.37
45.0000	0.0731	0.0731	0.30	0.0065	0.0065	-0.14	0.179E 05	0.180E 05	-0.16	0.201E-04	0.198E-04	1.69
50.0000	0.0765	0.0764	0.03	0.0063	0.0063	-0.01	0.175E 05	0.175E 05	-0.02	0.196E-04	0.192E-04	1.99
60.0000	0.0822	0.0826	-0.47	0.0061	0.0061	0.24	0.169E 05	0.169E 05	0.23	0.188E-04	0.183E-04	2.52
70.0000	0.0874	0.0882	-0.93	0.0059	0.0059	0.47	0.164E 05	0.163E 05	0.46	0.180E-04	0.175E-04	2.98
80.0000	0.0922	0.0934	-1.35	0.0058	0.0057	0.67	0.160E 05	0.158E 05	0.66	0.174E-04	0.169E-04	3.39
90.0000	0.0965	0.0982	-1.73	0.0056	0.0056	0.86	0.156E 05	0.154E 05	0.85	0.169E-04	0.163E-04	3.76
100.0000	0.1006	0.1027	-2.09	0.0055	0.0055	1.03	0.153E 05	0.151E 05	1.03	0.165E-04	0.158E-04	4.10

TABLE 3. - LOCATION AND MAGNITUDE OF SUBSURFACE ORTHOGONAL SHEAR STRESS CALCULATED BOTH NUMERICALLY AND WITH SIMPLIFIED FORMULAS

$[E' = 2.1972 \times 10^7 \ N/cm^2; \ F = 4.448 \ N; \ R_x = 1.0 \ cm]$

RADIUS OF CURVATURE RATIO, α	AUXILIARY PARAMETER			POSITION OF MAXIMUM SUBSURFACE ORTHOGONAL SHEAR STRESS						MAXIMUM SUBSURFACE ORTHOGONAL SHEAR STRESS (N/cm^2)		
				SURFACE POSITION (CM.)			DEPTH BELOW SURFACE (CM.)					
	t	$\bar{t}$	PERCENT ERROR, e	x_0	$\bar{x}_0$	PERCENT ERROR, e	z_0	$\bar{z}_0$	PERCENT ERROR, e	τ_0	$\bar{\tau}_0$	PERCENT ERROR, e
0.0100	5.7180	7.0026	-22.47	0.0820	0.0867	-5.81	0.464E-02	0.356E-02	23.23	0.642E 03	0.486E 03	24.26
0.0200	4.4236	4.8603	-9.87	0.0589	0.0602	-2.18	0.503E-02	0.442E-02	12.23	0.102E 04	0.910E 03	11.18
0.0300	3.8105	3.9815	-4.49	0.0481	0.0482	-0.18	0.524E-02	0.489E-02	6.78	0.134E 04	0.128E 04	4.73
0.0400	3.4304	3.4528	-1.51	0.0415	0.0411	1.12	0.538E-02	0.519E-02	3.54	0.161E 04	0.160E 04	0.95
0.0500	3.1639	3.1528	0.35	0.0362	0.0362	2.03	0.547E-02	0.539E-02	1.45	0.186E 04	0.189E 04	-1.44
0.0600	2.9631	2.9165	1.58	0.0335	0.0326	2.69	0.554E-02	0.554E-02	0.04	0.209E 04	0.215E 04	-3.02
0.0700	2.8048	2.7369	2.42	0.0308	0.0298	3.18	0.559E-02	0.564E-02	-0.95	0.230E 04	0.240E 04	-4.10
0.0800	2.6755	2.5949	3.01	0.0286	0.0276	3.56	0.563E-02	0.572E-02	-1.64	0.250E 04	0.262E 04	-4.84
0.0900	2.5673	2.4793	3.43	0.0268	0.0257	3.84	0.566E-02	0.578E-02	-2.13	0.269E 04	0.284E 04	-5.35
0.1000	2.4750	2.3829	3.72	0.0252	0.0242	4.06	0.568E-02	0.582E-02	-2.47	0.287E 04	0.303E 04	-5.69
0.2000	1.9632	1.8867	3.90	0.0168	0.0161	4.45	0.570E-02	0.585E-02	-2.70	0.432E 04	0.457E 04	-5.66
0.3000	1.7321	1.6825	2.86	0.0131	0.0126	3.80	0.560E-02	0.569E-02	-1.56	0.543E 04	0.566E 04	-5.33
0.4000	1.5946	1.5661	1.79	0.0110	0.0106	2.95	0.547E-02	0.560E-02	-0.45	0.634E 04	0.653E 04	-3.07
0.5000	1.5017	1.4890	0.85	0.0095	0.0093	2.10	0.533E-02	0.531E-02	0.48	0.712E 04	0.726E 04	-2.01
0.6000	1.4342	1.4335	-0.05	0.0085	0.0084	1.30	0.520E-02	0.520E-02	1.21	0.782E 04	0.790E 04	-1.11
0.7000	1.3825	1.3911	-0.62	0.0077	0.0077	0.55	0.507E-02	0.513E-02	1.78	0.845E 04	0.848E 04	-0.33
0.8000	1.3416	1.3575	-1.19	0.0071	0.0071	-0.14	0.494E-02	0.498E-02	2.21	0.902E 04	0.899E 04	0.35
0.9000	1.3080	1.3300	-1.66	0.0066	0.0066	-0.77	0.483E-02	0.483E-02	2.53	0.956E 04	0.947E 04	0.96
1.0000	1.2808	1.3070	-2.05	0.0061	0.0062	-1.36	0.472E-02	0.470E-02	2.76	0.101E 05	0.990E 04	1.51
1.2500	1.2287	1.2628	-2.78	0.0057	0.0059	-1.94	0.481E-02	0.459E-02	3.69	0.963E 04	0.952E 04	1.39
1.5000	1.1920	1.2307	-3.25	0.0055	0.0056	-2.41	0.486E-02	0.463E-02	4.24	0.929E 04	0.917E 04	1.31
1.7500	1.1649	1.2061	-3.54	0.0052	0.0054	-2.77	0.489E-02	0.466E-02	4.54	0.900E 04	0.889E 04	1.23
2.0000	1.1440	1.1865	-3.71	0.0050	0.0052	-3.05	0.484E-02	0.466E-02	4.68	0.875E 04	0.865E 04	1.14
3.0000	1.0937	1.1350	-3.78	0.0045	0.0047	-3.55	0.474E-02	0.455E-02	4.52	0.801E 04	0.795E 04	0.77
4.0000	1.0681	1.1049	-3.45	0.0042	0.0044	-3.59	0.463E-02	0.452E-02	3.93	0.752E 04	0.749E 04	0.42
5.0000	1.0528	1.0847	-3.03	0.0040	0.0043	-3.43	0.453E-02	0.448E-02	3.26	0.715E 04	0.715E 04	-0.12
6.0000	1.0427	1.0700	-2.62	0.0038	0.0041	-3.21	0.444E-02	0.441E-02	2.64	0.687E 04	0.688E 04	-0.13
7.0000	1.0356	1.0588	-2.24	0.0037	0.0039	-2.97	0.436E-02	0.435E-02	2.08	0.664E 04	0.666E 04	-0.33
8.0000	1.0304	1.0501	-1.91	0.0035	0.0038	-2.73	0.428E-02	0.429E-02	1.59	0.645E 04	0.648E 04	-0.49
9.0000	1.0264	1.0430	-1.61	0.0035	0.0036	-2.51	0.421E-02	0.423E-02	1.17	0.628E 04	0.632E 04	-0.62
10.0000	1.0233	1.0372	-1.35	0.0033	0.0035	-2.30	0.394E-02	0.418E-02	0.81	0.614E 04	0.618E 04	-0.73
15.0000	1.0143	1.0195	-0.50	0.0031	0.0031	-1.00	0.359E-02	0.395E-02	-0.33	0.562E 04	0.568E 04	-0.97
20.0000	1.0102	1.0111	-0.09	0.0029	0.0029	-0.66	0.347E-02	0.377E-02	-0.79	0.529E 04	0.534E 04	-0.88
25.0000	1.0078	1.0066	0.12	0.0027	0.0028	-0.22	0.337E-02	0.362E-02	-0.93	0.505E 04	0.509E 04	-0.75
30.0000	1.0062	1.0041	0.21	0.0026	0.0027	-0.05	0.329E-02	0.350E-02	-0.82	0.486E 04	0.490E 04	-0.60
35.0000	1.0052	1.0026	0.26	0.0025	0.0026	-0.21	0.321E-02	0.340E-02	-0.69	0.471E 04	0.474E 04	-0.45
40.0000	1.0039	1.0017	0.27	0.0025	0.0025	-0.44	0.315E-02	0.331E-02	-0.55	0.458E 04	0.460E 04	-0.30
45.0000	1.0034	1.0011	0.26	0.0024	0.0025	-0.64	0.304E-02	0.323E-02	-0.40	0.447E 04	0.449E 04	-0.16
50.0000	1.0027	1.0008	0.24	0.0023	0.0024	-0.82	0.296E-02	0.316E-02	-0.11	0.438E 04	0.438E 04	-0.11
60.0000	1.0023	1.0004	0.21	0.0022	0.0023	-0.99	0.288E-02	0.305E-02	-0.15	0.422E 04	0.422E 04	-0.35
70.0000	1.0020	1.0002	0.19	0.0022	0.0022	-1.15	0.282E-02	0.295E-02	0.39	0.409E 04	0.408E 04	0.57
80.0000	1.0017	1.0001	0.17	0.0022	0.0022		0.288E-02	0.287E-02	0.61	0.398E 04	0.396E 04	0.77
90.0000	1.0015	1.0000	0.15	0.0021	0.0021		0.282E-02	0.280E-02	0.81	0.389E 04	0.386E 04	0.95
100.0000	1.0015	1.0000		0.0021	0.0021		0.276E-02	0.274E-02		0.381E 04	0.378E 04	

TABLE 4. – SIMPLIFIED EQUATIONS
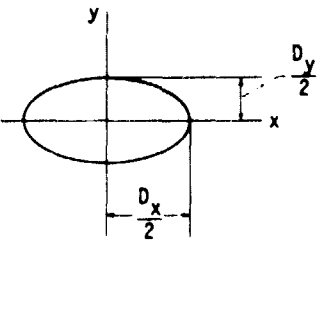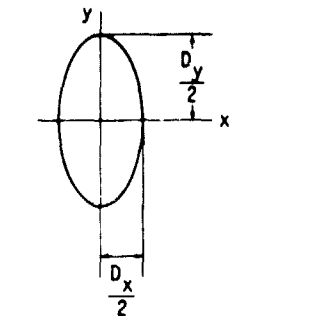
(diagram of horizontal ellipse with $\frac{D_y}{2}$ and $\frac{D_x}{2}$)	(diagram of vertical ellipse with $\frac{D_y}{2}$ and $\frac{D_x}{2}$)
$1 \leq \alpha \leq 100$	$0.01 \leq \alpha \leq 1$
$\bar{k} = \alpha^{2/\pi}$	$\bar{k} = \alpha^{2/\pi}$
$\bar{\mathcal{F}} = \frac{\pi}{2} + q \ln \alpha$	$\bar{\mathcal{F}} = \frac{\pi}{2} - q \ln \alpha$
where $q = \frac{\pi}{2} - 1$	where $q = \frac{\pi}{2} - 1$
$\bar{\mathcal{E}} = 1 + \frac{q}{\alpha}$	$\bar{\mathcal{E}} = 1 + q\alpha$
$D_y = 2 \left(\frac{6k^2 \mathcal{E} FR}{\pi E'} \right)^{1/3}$	$D_y = 2 \left(\frac{6k \mathcal{E} FR}{\pi E'} \right)^{1/3}$
where $R^{-1} = R_x^{-1} + R_y^{-1}$	where $R^{-1} = R_x^{-1} + R_y^{-1}$
$D_x = 2 \left(\frac{6 \mathcal{E} FR}{\pi k E'} \right)^{1/3}$	$D_x = 2 \left(\frac{6 \mathcal{E} FR}{\pi E' k^2} \right)^{1/3}$
$\delta = \mathcal{F} \left[\left(\frac{4.5}{\mathcal{E} R} \right) \left(\frac{F}{\pi k E'} \right)^2 \right]^{1/3}$	$\delta = \mathcal{F} \left[\left(\frac{4.5}{\mathcal{E} R} \right) \left(\frac{Fk}{\pi E'} \right)^2 \right]^{1/3}$
$\bar{t} = 1 + 0.16 \ \mathrm{csch} \left(\frac{\bar{k}}{2} \right)$	$\bar{t} = 1 + 0.16 \ \mathrm{csch} \left(\frac{\bar{k}}{2} \right)$
$\tau_0 = \sigma_{max} \frac{\sqrt{2t - 1}}{2t(t + 1)}$	$\tau_0 = \sigma_{max} \frac{\sqrt{2t - 1}}{2t(t + 1)}$
$z_0 = \frac{D_x}{2(t + 1) \sqrt{2t - 1}}$	$z_0 = \frac{D_x}{2(t + 1) \sqrt{2t - 1}}$
$x_0 = \pm \frac{t}{t + 1} \sqrt{\frac{2t + 1}{2t - 1}} \frac{D_x}{2}$	$x_0 = \pm \frac{t}{t + 1} \sqrt{\frac{2t + 1}{2t - 1}} \frac{D_x}{2}$

TABLE 5. - PRACTICAL APPLICATIONS FOR DIFFERING CONFORMITIES

$$[E' = 2.197 \times 10^7 \text{ N/cm}^2.]$$

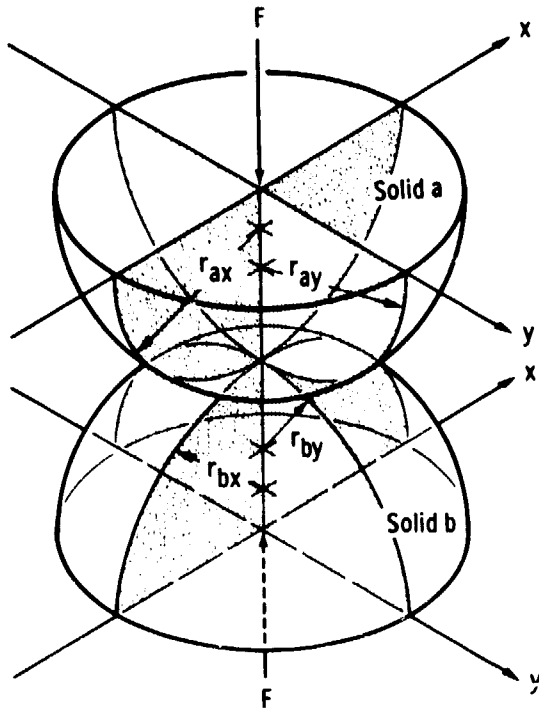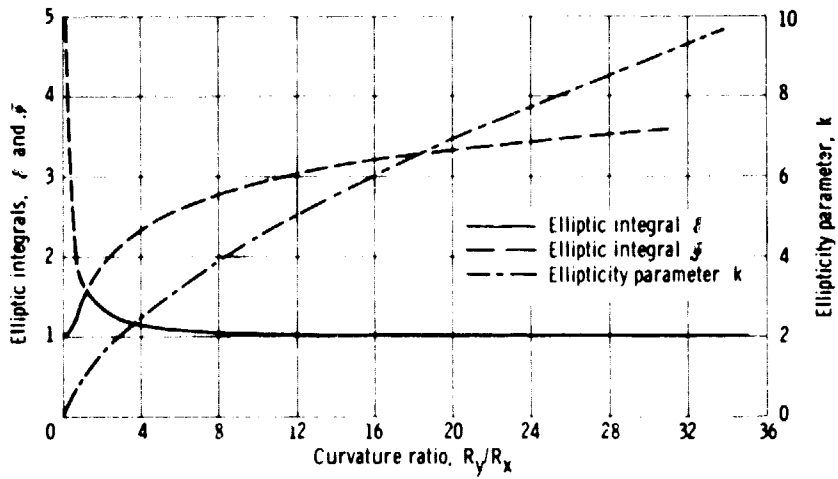| CONTACT PARAMETERS	WHEEL ON RAIL	BALL ON PLANE	BALL - OUTER-RING CONTACT
F	1.00×10^5 N	222.4111 N	222.4111 N
r_{ax}	50.1900 cm	0.6350 cm	0.6350 cm
r_{ay}	∞	0.6350 cm	0.6350 cm
r_{bx}	∞	∞	-3.8900 cm
r_{by}	30.0000 cm	∞	-0.6600 cm
a	0.5977	1.0000	22.0905
k	0.7099	1.0000	7.3649
$\bar{k}$	0.7206	1.0000	7.1738
ℓ	1.3526	1.5708	1.0267
$\bar{\ell}$	1.3412	1.5708	1.0258
$\mathscr{f}$	1.8508	1.5708	3.3941
$\bar{\mathscr{f}}$	1.8645	1.5708	3.3375
D_y	1.2801 cm	0.0426 cm	0.1842 cm
$\bar{D}_y$	1.2829 cm	0.0426 cm	0.1810 cm
D_x	1.8032 cm	0.0426 cm	0.0250 cm
$\bar{D}_x$	1.7802 cm	0.0426 cm	0.0252 cm
δ	0.0089 cm	7.13×10^{-4} cm	3.56×10^{-4} cm
$\bar{\delta}$	0.0091 cm	7.13×10^{-4} cm	3.57×10^{-4} cm
σ_{max}	8.27×10^4 N/cm^2	2.34×10^5 N/cm^2	9.22×10^4 N/cm^2
$\bar{\sigma}_{max}$	8.36×10^4 N/cm^2	2.34×10^5 N/cm^2	9.30×10^4 N/cm^2
t	1.4354	1.2808	1.0090
$\bar{t}$	1.4346	1.3070	1.0089
x_0	± 0.8862 cm	± 0.0195 cm	± 0.0096 cm
$\bar{x}_0$	± 0.8745 cm	± 0.0197 cm	± 0.0097 cm
z_0	0.5410 cm	0.0149 cm	0.0123 cm
$\bar{z}_0$	0.5350 cm	0.0145 cm	0.0124 cm
τ_0	1.62×10^4 N/cm^2	5.01×10^4 N/cm^2	2.29×10^4 N/cm^2
$\bar{\tau}_0$	1.64×10^4 N/cm^2	4.94×10^4 N/cm^2	2.32×10^4 N/cm^2

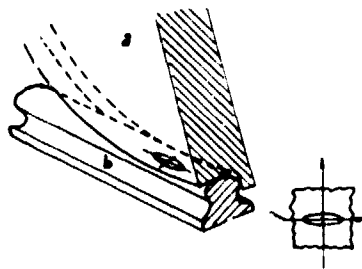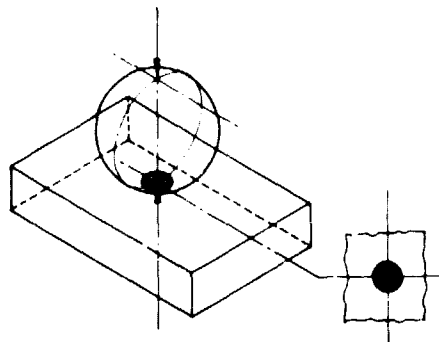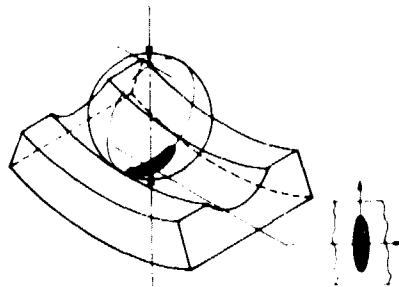Figure 1. - Geometry of contacting elastic solids.

Figure 2. - Ellipticity parameter and elliptic integrals of first and second kinds as a function of curvature ratio.

(a) Wheel on rail.

(b) Ball on plane.

(c) Ball - outer-ring contact.

Figure 3. - Three degrees of conformity.